applied sciences

MDPI

Article

A Study on Power Transmission Control for Applying MR Fluid Multi-Plate Clutch to Automobile Power Distribution Device

Jin-Young Park [1], Jae-Hoon Jeon [2] and Young-Choon Kim [3,*]

[1] EPSTech Co., Ltd., Daejeon 34202, Republic of Korea; pjy0079@epstech.co.kr
[2] Korea Automotive Technology Institute, Cheonan 31214, Republic of Korea; jhjeon@sktech.re.kr
[3] Department of Intelligent Mobility Engineering, Kongju National University, Cheonan 32439, Republic of Korea
* Correspondence: yckim59@kongju.ac.kr; Tel.: +82-41-521-9274

Abstract: The aim of this study is to design and manufacture a multi-plate clutch system that uses magnetorheological (MR) fluid control to allow for a variable power transmission ratio in power distribution systems. MR fluid is a smart material that enables presenting a solution to the shocks and power loss that occur due to mechanical problems in power distribution systems. As such, the longitudinal and lateral dynamic properties of 4WD (four-wheel drive) vehicles were examined and analyzed to develop an algorithm to control the front/rear power distribution according to the road surface state and driving conditions. To verify the algorithm, the CarSim vehicle dynamics simulation program was adopted to perform experiments to understand the vehicle's dynamic performance improvements and turning stability via a HILS (Hardware in the Loop) system. In this study, an MR fluid, multi-plate clutch was used that combines a dry clutch and a wet clutch using the characteristics of the MR fluid. Such a clutch was designed to enable continuous and smooth torque transmission by utilizing the strengths of each of the dry and wet clutches. The CarSim vehicle dynamics program was used to conduct the experiments, which were conducted by linking to the manufactured MR fluid clutch experimental device. The experiments investigated the dynamic performance based on the power distribution ratio by performing longitudinal flat, inclined driving and lateral DLC (double lane change) driving. In summary, this study found that it is possible to perform power transmission by applying a current to an MR fluid and forming a magnetic field to change the flow properties of the fluid to control the torque transmission ratio that occurs in an MR fluid clutch.

Keywords: MR fluid; multi-plate clutch; four-wheel drive; power transmission

Citation: Park, J.-Y.; Jeon, J.-H.; Kim, Y.-C. A Study on Power Transmission Control for Applying MR Fluid Multi-Plate Clutch to Automobile Power Distribution Device. *Appl. Sci.* **2024**, *14*, 3871. https://doi.org/10.3390/app14093871

Academic Editor: Mickaël Lallart

Received: 11 March 2024
Revised: 20 April 2024
Accepted: 23 April 2024
Published: 30 April 2024

1. Introduction

Four-wheel drive (4WD) vehicles were originally developed for military use to drive on unpaved or rough roads. However, as passenger vehicle development becomes an increasingly active field, various 4WD (four-wheel drive) systems are being developed. The representative power distribution devices that have been applied to 4WD vehicles include viscous coupling and transfer cases. Viscous coupling, which is mainly used in front-wheel-based 4WD vehicles, has the advantage of low noise and excellent durability because it uses oil to transmit power. However, since power is transmitted only using friction due to the viscosity of oil, the maximum power transmission value is low, and the response is slow compared to the mechanical friction transmission method.

In addition, the gear-driven and chain-driven types of transfer cases, which are mainly used in rear-wheel-based 4WD vehicles, are filled with lubricant to improve friction and heat generation inside the transfer case, but shock does occur during power transmission. Prior to this study, various other studies were conducted as detailed below [1–3].

Studies have been conducted on the slip control of the clutch to increase the power transmission efficiency between the clutch and driveshaft, as well as to reduce the shock that occurs during engagement. Kim et al. proposed a clutch slip control logic that uses

an automatic transmission torque converter, and they verified its performance using a simulator [4]. Moreover, Kim et al. also proposed various control algorithms for reducing slip in dry clutches that are used in Semi-Automatic Transmission, and they improved engagement performance relative to the conventional method [5].

Currently, studies are being conducted to mitigate the shocks and friction that occur during clutch engagement. Jo et al. studied properties that can increase power transmission efficiency by analyzing the effect of parameters that can lessen the dynamic behavior of the clutch torque and friction properties based on the pressure conditions in the clutch engagement process of a DCT (Dual Clutch Transmission) [6]. Gam et al. developed a transmission algorithm for reducing hydraulic clutch shocks and optimizing the transmission time. Accordingly, they developed a transmission controller by analyzing clutch properties, as well as hydraulic valve properties [7]. In addition, studies are being conducted on control algorithms for developing and using torque distribution system controllers to understand the vehicle's driving state in real time and the appropriate distribution of power. Park et al. developed an algorithm for the operation of a torque distribution system's solenoid valve to improve dynamic performance, and they proved its feasibility by utilizing it in an actual vehicle [8].

Unlike 2WD (two-wheel drive) vehicles, 4WD vehicles use a power distribution system to transmit the driving force to the four wheels. Generally, 4WD vehicles have excellent longitudinal and lateral driving stability that enable them to traverse different road surface conditions. Numerous automobile manufacturers are conducting studies to overcome the disadvantages of 4WD and improve power efficiency.

Research has been conducted to improve performance by applying MR fluids to automobile power transmission systems. Shuyou Wang et al. proposed a shear-mode MR clutch with a uniform magnetic field distribution along the radial direction for a tension control system based on a detailed analysis of the axial magnetic induction intensity generated by the coil along the radial distribution [9]. Jie Wu et al. presented a new design of a multipole magnetorheological (MR) clutch with hybrid magnetization using multiple permanent magnets and multiple excitation coils [10]. Enrico Galvagno et al. proposed a new methodology for evaluating dual-clutch transmission vibrations during gear shifting. Experimental tests were performed on the basis of the ability to predict, through numerical simulations, the oscillatory behavior of the gearbox, i.e., a typical dynamic quantity used to objectively evaluate the acceleration of the points on the outer surface of the gearbox housing [11]. Manish Kumar Thakur et al., using simulation techniques and experimental studies, created a new seal for an outer radius that is designed to improve the torque transmission of a magnetorheological clutch, and the transmitted torque was measured and studied for improvement [12]. Anurag Singh et al. designed a new drum magnetorheological clutch with a wedge-shaped boundary, and experimental results showed that the proposed wedge-shaped drum magnetorheological clutch generated more torque than the existing drum magnetorheological clutch, thus resulting in better performance [13]. M. D. Christie et al. proposed a magnetorheological fluid-based differential (planetary) gear transmission that variably connects motor power to a load attached to the planetary carrier output through a sun gear input [14]. Cirimele and Vincenzo et al. proposed the study of magnetic gears through multi-objective optimization. A multi-objective optimization approach was proposed to maximize the transmitted torque per unit mass of the magnetic gears while minimizing the moment of inertia of the moving parts. Self-performance optimization is a deterministic optimization algorithm combined with a weighted-sum approach of objectives, and the results were discussed and compared with those of commercial applications [15]. Mattia Filippini et al. proposed a magnetic gear (MG) that achieves the same functions as a differential while having unique advantages such as reduced maintenance and high efficiency, and they verified it through experiments and simulations [16]. Many studies have been conducted on power transmission devices using MR fluid in automobiles, but most of them involve the power transmission using only the sheer force of the MR fluid;

thus, there has been no research conducted that addresses power transmission through mechanical friction [17–19].

In this paper, based on a detailed analysis of the axial magnetic induction intensity generated by the coil along the radial distribution, a shear-mode MR (magnetorheological) clutch with uniform magnetic field distribution along the radial direction is proposed for a tension control system.

MR fluid is a smart material that provides a solution to mechanical problems in power distribution systems. Accordingly, the longitudinal and lateral dynamic properties of 4WD vehicles were examined and analyzed, and an algorithm was developed to control the front/rear power distribution using an MR fluid multi-plate clutch according to the road surface state and driving conditions. The CarSim vehicle dynamics simulation program was used to check the performance of the algorithm by conducting vehicle dynamic performance and turning stability experiments using a HILS (Hardware in the Loop) system.

2. Theory and Experimental Method

2.1. MR Fluid Power Distribution System

2.1.1. MR Fluid Properties

MR fluid experiences an MR effect where the fluid flow's resistance increases under a magnetic field load, and paramagnetic particles are dispersed in a solvent with low permeability. In the absence of a magnetic field load, the MR fluid behaves like a Newtonian fluid, where the particles move freely; however, when a magnetic load is applied, the particles become charged and form a chain structure, exhibiting the behavior of a Bingham fluid that has yield stress. Generally, the rheological properties of an MR fluid change according to the strength of the magnetic field. Accordingly, τ denotes the shear stress of the MR fluid, and it can be predicted based on the MRF's Bingham model, as shown in the equation below [20].

$$\tau = \tau_y + \eta\dot{\gamma}. \tag{1}$$

Here, τ_y and η denote the MR fluid's yield stress and viscosity coefficient after yielding, and $\dot{\gamma}$ denotes the shear rate of the MR fluid at the interface. Since the gap between the disc and the plate is very small, it can be assumed that the MR fluid's shear rate at the interface is distributed linearly, and it can be determined as shown below.

$$\dot{\gamma} = \frac{r\omega}{d}. \tag{2}$$

Here, r and d denote the radius of the disc's smallest area and the space between the disc and the plate, respectively, and ω symbolizes the angular velocity difference between the disc and the plate. The shear stress of the MR fluid indicates the shear stress of the fluid when a magnetic field is applied from the outside. The fluid's flow begins shortly and behaves in a complex manner; therefore, it is difficult to accurately measure the yield shear stress. Accordingly, linear equations for the shear rate and the shear stress are found, and the shear stress when the shear rate is zero is defined as the dynamic yield stress. Generally, the dynamic yield stress is treated as the MR fluid's yield shear stress, and it is expressed as a function of the magnetic field's strength.

The dynamic yield stress is found, as shown in Equation (3), using a model in which viscosity is affected by the magnetic field strength. The approximate formula constants found here include characteristic eigenvalues that are determined by the solvent used in the MR fluid, the type of particles, the composition ratio, and the composition environment. The MRF-132DG fluid's intrinsic property values are listed in Table 1 [17,18].

$$Y = Y_\infty + (Y_0 - Y_\infty)\left(2e^{-B\sigma_{SY}} - e^{-2B\sigma_{SY}}\right). \tag{3}$$

Here, Y_∞, Y_0, B, and σ_{SY} correspond to the MRF's magnetic field saturation state, the magnetic field removal state, the magnetic density applied to the MRF, and the saturated moment, respectively.

For MR fluids, the viscosity coefficient and yield stress must be calculated separately. This can be obtained through the parameters listed in Table 1 and Equation (3). The viscosity coefficient can be obtained through the saturated viscosity coefficient η_∞, the natural viscosity coefficient η_0, and the viscosity coefficient saturation moment $\sigma_{S\eta}$ in the Y term of Equation (3). The yield stress can be obtained through the saturated yield stress $\tau_{y\infty}$, the natural yield stress τ_{y0}, and the yield saturation in the Y term can be obtained with the saturation moment $\sigma_{S\tau_y}$ [19].

Table 1. The rheological properties of the MRF-132DG fluid.

Parameter	Value
η_0	0.1 Pa·s
η_∞	3.8 Pa·s
$\sigma_{S\eta}$	4.5 T^{-1}
τ_{y0}	12 Pa
$\tau_{y\infty}$	40,000 Pa
$\sigma_{S\tau_y}$	2.9 T^{-1}

2.1.2. MR Fluid Multi-Plate Clutch Design

Friction clutches create power transmission through engagement between the disc and the plate that connect the power and the load. There are two clutch types, including dry clutches and wet clutches.

Dry clutches have the disadvantages of poor durability, noise, vibration, and overheating due to the shocks that occur during engagement; however, they are small, light, and have excellent power transmission efficiency. In contrast, wet clutches are large, heavy, and have low transmission efficiency owing to the oil in their interiors. However, they experience smaller shocks than dry clutches during engagement; therefore, they have less noise and vibration, and they also have excellent durability [20].

Applying MR fluid between rotating discs can effectively dampen the vibrations of the rotor. Therefore, applying MR fluid to a multi-plate clutch will effectively reduce vibrations. The MR (magnetorheological) fluid multi-disc clutch, as illustrated in Figure 1, is designed to combine the characteristics of both dry and wet clutches, thus enabling continuous and smooth engagement.

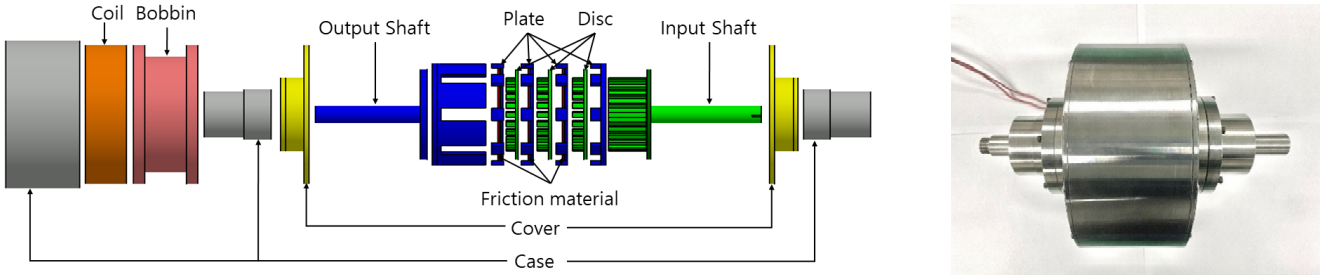

(**a**) (**b**)

Figure 1. Diagram of the MR fluid multi-plate clutch. (**a**) An exploded CAD model of an MR fluid multi-plate clutch. (**b**) Prototype MR fluid multi-plate clutch.

First, it is a friction mode that transmits power using a friction force generated by the contact between the input and output shaft friction surfaces, like regular dry friction clutches. This friction mode can generate maximum torque, but a significant impact also occurs when the plates are in contact with each other. Second, it has a fluid mode. Unlike conventional fluid couplers that deliver power using the viscous force of the fluids in the plates, it transmits power using an MRF whose shear stress varies with the magnetic field intensity. Considering the above, the MR fluid multi-plate clutch was designed, as shown

in Figure 1. For more details, including the detailed geometry of the MR clutch, see the authors' previous research [19].

2.1.3. MR Fluid Properties

Generally, the modes of operation in which the properties of the MR fluid are applied to the clutch mechanism can be divided into two: friction mode and fluid mode. Friction mode transmits power by making contact between the disc and the plate-like dry clutch, whereas fluid mode transmits power through the shear stress of the MR fluid, which changes according to the strength of the external magnetic field, thereby reducing noise and vibration.

A multi-plate clutch has N number of friction surfaces; however, its size and weight are different than those of a single-plate clutch. However, it was assumed that these values are the same to simplify the mathematical proof, and the torque modeling of a single-plate clutch was performed to design the MR multi-plate clutch. A single-plate clutch comprises an input shaft and an output shaft, and it is assumed that there is a friction pad between them. Moreover, F denotes the input value in friction mode.

The transmitted torque of the clutch can be found through a torque modeling equation, as well as through the axial clamping force that acts on the clutch plate cross-section, as shown in Equation (4):

$$F = \int_{r_i}^{r_o} 2\pi r p dr = \pi p(r_o^2 - r_i^2), \tag{4}$$

where p denotes the pressure that acts on the friction pad cross-section during clutch contact (this pressure was assumed to act consistently per unit area), and r_i and r_o denote the inner and outer diameter of the clutch friction pad.

The transmission torque T_M caused by the contact pressure between the plates in a single-plate clutch is shown in Equation (5).

$$T_M = \iint_{r_i}^{r_o} r\mu \; sgn(\omega) dF dr = \frac{2\pi\mu p}{3}\left(r_o^3 - r_i^3\right) sgn(\omega) = \frac{2F\mu\left(r_o^3 - r_i^3\right)}{3\left(r_o^2 - r_i^2\right)} sgn(\omega), \tag{5}$$

where μ denotes the friction coefficient of the clutch friction pad, and it is defined as a function of the plate's angular velocity ω and pressure p. For more details, refer to the authors' previous study [18].

2.1.4. Multi-Plate Clutch Fluid Mode Torque Modeling

Magnetic field control torque refers to the torque that is transmitted by the MR fluid between the friction surface of the input and output shaft, and there is a torque that is transmitted by viscosity and a torque that is transmitted by the magnetic field. The torque transmitted by the magnetic field is the MRF's friction, which acts upon the surface between the disc, the plate, and the external annular part. The MR single-plate clutch's magnetic control torque T_{MR} is caused by the magnetic field and is determined by the MR fluid's yield shear stress τ_y and the friction area, and it can be derived from the MRF, as shown in Equation (6).

$$T_{MR} = \int_A \tau r dA = 2\pi \int_{r_i}^{r_o} \tau r^2 dr. \tag{6}$$

The MR fluid used in this study is MRF-132DG from the LORD Company (Cary, NC, USA). In a MR multi-plate clutch, shear stress affects the MR fluid at the end annular part of the disc and plate. The average magnetic flux density, which is calculated using numerical integration and is similar to that in the cross-sectional space of the MR fluid, allows us to derive the following equation (this equation assumes that the shear rate of the MR fluid is linearly distributed):

$$T_{th} = 2\pi r^2 l\left(\tau_y + \eta\frac{r\omega}{d}\right), \tag{7}$$

where l and r denote the annular part's radius and length. The transmission equation of the MR single clutch in the magnetic field off mode (when a magnetic field is not applied to the MR fluid) is as follows.

$$T_0 = \frac{\pi\eta_0}{h}\left(r_o^4 - r_i^4\right)\omega + \frac{4\pi\tau_{y0}}{3}\left(r_o^3 - r_i^3\right) + 2\pi r_o^2 t_d(\tau_{y0} - \eta_0\frac{r_o\omega}{h}). \quad (8)$$

Here, h refers to the gap between disks, and t_d refers to the thickness of the disk and plate. The torque calculation equations for the single-plate clutch can be used to determine the torque modeling equation for the multi-plate clutch that is to be designed. Since the MR multi-plate clutch has N number of friction surfaces, the multi-plate clutch's mode transmission torque T_{M_m} can be expressed as shown in Equation (9). However, in the fluid mode, torque transmission is performed by the MR fluid between the discs and the plates; therefore, it is necessary to compute the torque values at all locations. Accordingly, the fluid mode transmission torque T_{MR_m} is the value obtained by adding all the torque values acting on the spaces between the discs and the plates, as shown in Equation (10).

$$T_{M\_m} = T_M + T_0, \quad (9)$$

$$T_{MR\_m} = \sum_{I=0}^{n}\{T_{MR} + T_{th} + T_0\}. \quad (10)$$

Here, n denotes the number of spaces between the discs and the plates. In the torque calculation equation, the transmission torque of the MR friction clutch can be obtained by ignoring the torque caused by the friction of the sealing and the bearings [19,21,22].

2.2. 4WD Vehicle Dynamic Properties Analysis

In this study, power from the FF 4WD vehicle's engine and transmission is transmitted to the rear wheel driveshaft and the rear wheels using the power distribution system, and the vehicle is driven in a full-time 4WD style. The CarSim simulation was used to change the road surface conditions and the power distribution ratio of the front/rear wheels to confirm the proper torque distribution ratio of the front/rear wheels among the 4WD vehicle's lateral/longitudinal properties (Table 2).

Table 2. The CarSim vehicle model's specifications.

Parameter	Value
Vehicle classification	E-Segment
Internal Engine Model, kW	200
Transmission	6-Speed
Sprung Mass, kg	1590
Unsprung Mass, kg	270
Wheelbase Length, mm	2950
Length, mm	4770
Width, mm	1875
Height, mm	1800
Tire Model	265/75 R16
Center of Gravity mm	650

2.2.1. Longitudinal Driving Performance

Generally, the longitudinal driving performance is determined by the vehicle's driving force, which is determined by the friction force between the road surface and the wheel. Typically, a full-time 4WD vehicle equally distributes the driving force to the four wheels, thereby providing better traction and stability than a part-time 4WD vehicle. Moreover, since the vehicle load applied to the front/rear wheels varies according to the engine position, a torque distribution that is suitable for the vehicle load is required [23–26].

The vehicle's acceleration performance and climbing performance were checked to analyze the longitudinal driving performance. First, a road with a 0% gradient in the

longitudinal direction was set up to check the vehicle's acceleration performance, and the road environment was configured as shown in Figure 2. The time taken for the vehicle to go from 0 to 100 km/h was compared, and the vehicle's acceleration performance according to the power distribution ratio was checked.

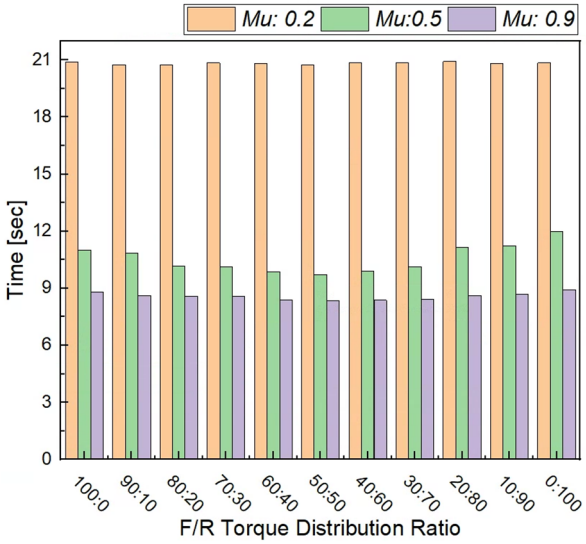

Figure 2. Simulation results for the acceleration performance during lateral driving.

The front/rear power distribution ratios of 60:40, 50:50, and 40:60 indicated relatively good acceleration performance and climbing performance in the simulation results of the longitudinal driving performance. In a 4WD vehicle, the acceleration performance is approximately 1.06 times better than that of a front-wheel or rear-wheel drive vehicle, and the climbing performance is approximately 1.16 times better on average. During rapid acceleration, the vehicle's center of gravity shifts toward the rear of the vehicle, and driving resistance occurs in the opposite direction to the vehicle's direction of travel; therefore, performance differences occur according to the power distribution ratio. Consequently, a 4WD vehicle's power distribution ratio has an effect on its longitudinal driving performance, and there must be the proper distribution between the front and rear wheels [27–30].

2.2.2. Lateral Driving Performance

To evaluate the turning performance of the vehicle according to the drive style, CarSim was used to set up the driving state of the vehicle in a DLC (double-lane change) environment while driving at 80 km/h. Moreover, the lateral acceleration and yaw rate values of the vehicle were produced by the simulation, and the vehicle's turning performance was examined. Figure 3 illustrates graphs comparing the lateral acceleration and yaw rates according to the drive style of the vehicle.

The lateral driving performance simulation results confirmed that the lateral acceleration and yaw rate values change according to the drive style of the vehicle. The results of comparing the lateral acceleration values according to the drive style of the vehicle showed that the RWD vehicle had the largest values, and the maximum difference was 1.05 times.

As a result of analyzing the rates of front-wheel drive vehicles and four-wheel drive vehicles in the DLC scenario, it was confirmed that a similar trend of approximately 98% was observed. However, in the case of rear-wheel drive vehicles, it was confirmed that the yaw rate differed by more than 10% in some sections compared to other vehicles. In a DLC scenario in which each driving method was tested, it was confirmed that the dynamic behavior of rear-wheel drive vehicles is unstable during emergency steering.

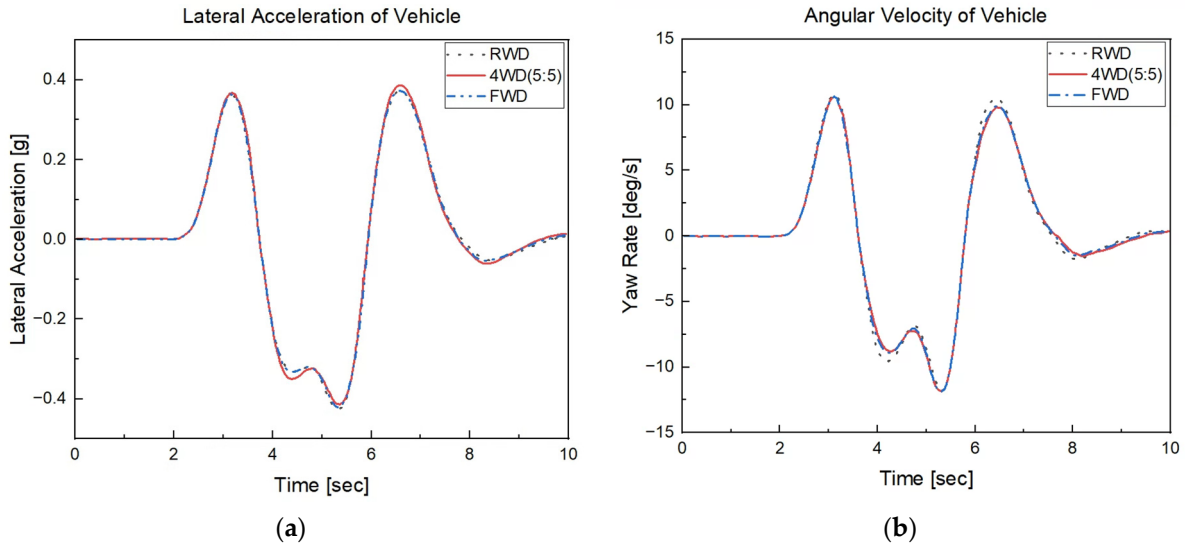

Figure 3. Comparison based on the vehicle drive style. (**a**) Comparison of the lateral acceleration according to the vehicle driving style. (**b**) Comparison of the yaw rate according to the vehicle driving style.

2.3. Experiment Method

2.3.1. Experiment Equipment

Figure 4 shows a schematic diagram of the experimental setup used to conduct the experiments in this study. The experimental setup consisted of a control board, synchronous motor, DC power supply, DAQ board, step motor, LM guide, MR fluid multi-plate clutch, torque sensor, and electronic brake.

A Doosan Company's (Seoul, Republic of Korea) PH50CA-1 5 kW synchronous motor was used to generate the driving force output from the vehicle's transmission, and the power transmission was linked to the clutch using 1:1 gears. Additionally, a step motor and LM guide were used to control the disc and plate distances and clamping force of the MR fluid multi-plate clutch.

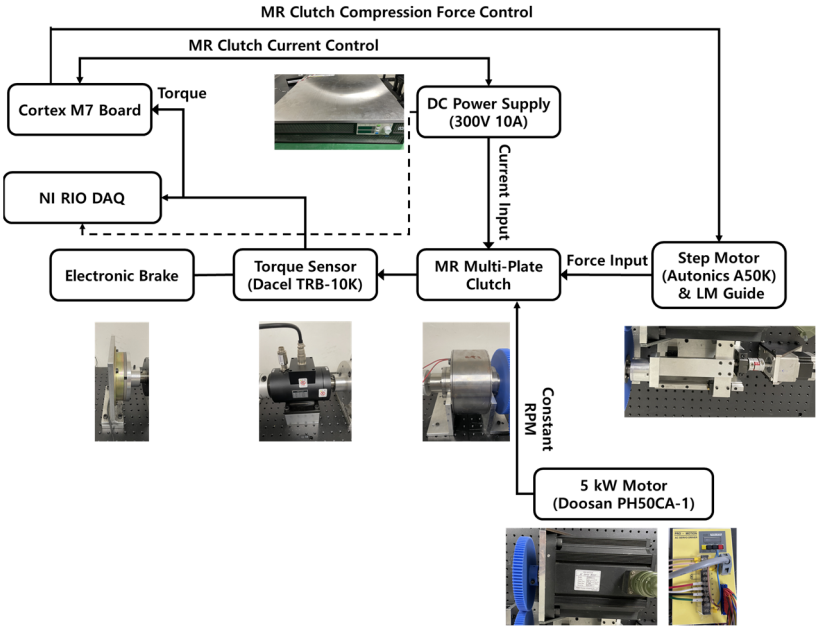

Figure 4. The HiLS system configuration.

2.3.2. Control System

Figure 5 illustrates a block diagram of the control system for the power distribution system that uses the MR fluid multi-plate clutch. As can be clearly seen, the front/rear power distribution ratio signals were output to a DAQ board that was connected to a computer using a controller that adapts to each of the driving conditions, which were designed in CarSim 2019 and MATLAB/Simulink.

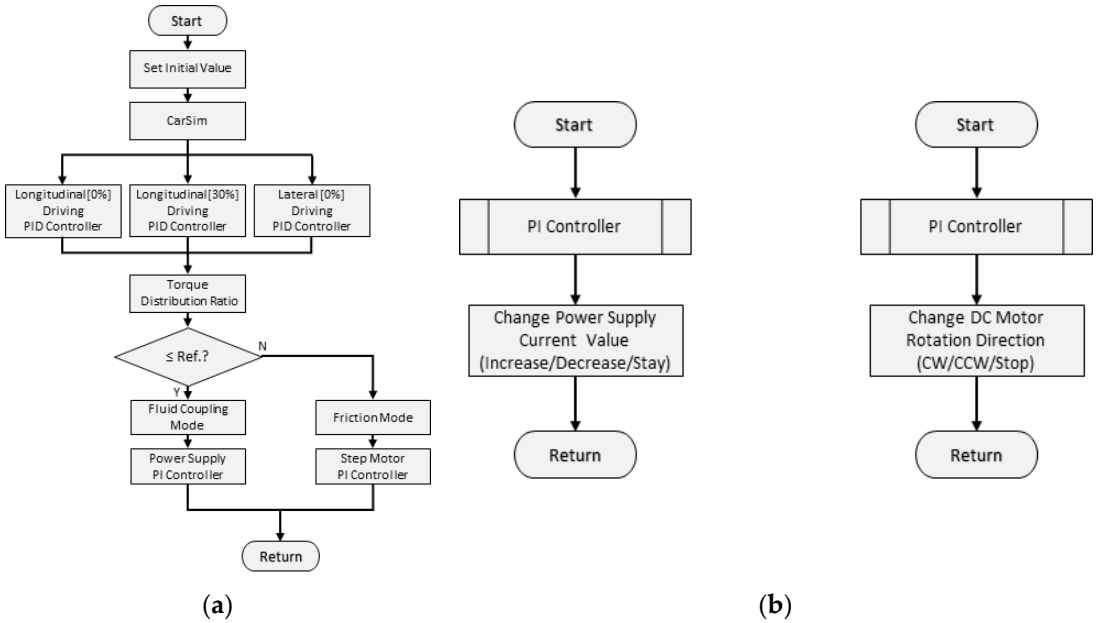

Figure 5. Control system flowchart. (**a**) Main routine. (**b**) Sub routine.

A circuit was configured to control the MR multi-plate clutch, and an STM32F767VGT6 microprocessor was employed to control the current and compression force.

The clutch torque values produced by the operation mode were calculated as proportional to the torque capacity of the CarSim vehicle model and inputted in the front/rear drive shafts of the vehicle to create a single power distribution system.

The clutch torque values produced by the operation mode were calculated as proportional to the torque capacity of the CarSim vehicle model and inputted in the front/rear drive shafts of the vehicle to create a single power distribution system. The clutch torque value was measured using a torque sensor and compared with a reference value obtained in the basic experiments. The torque value can be changed by changing the operating mode of the MR fluid multi-disc clutch.

If the measured torque value is less than or equal to the reference torque value, the MR fluid multi-disc clutch will operate in fluid mode using only current control; if it exceeds it, the step motor is positive and the drive goes in the reverse direction, and the distance between the clutch disc and plate is also adjusted to operate in friction mode.

The clutch torque value output in the operating mode is proportionally calculated according to the torque capacity of the CarSim vehicle model and input to the vehicle's front and rear drive shafts, thereby forming a one-power distribution device system. The control system's flowcharts are shown in Figure 5.

3. Experiment Results and Observations

3.1. Basic Experiment on Output Torque by Current and Drive RPM

To apply the fluid mode, the distance between the clutch's discs and plates was set to a maximum of 2 mm, and, for safety reasons, the rotational speed was increased in 40 rpm intervals from 20 to 100 rpm while the power supply's current value was increased in increments of 0.2 A from 0 to 2 A to examine the maximum transmission torque. The

results indicated that the torque increased in proportion to the current, and maximum torque values of 16.2, 16.6, and 16.7 Nm were obtained at a current of 2 A. The results are shown in Figure 6.

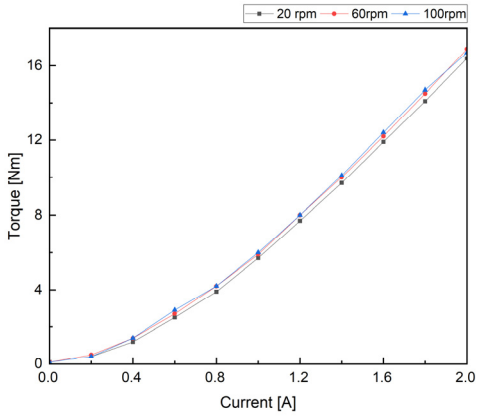

Figure 6. Graph of the torque by current value and drive RPM.

3.2. Simulation and HILS Experiment Results

3.2.1. Longitudinal Driving Simulation Conditions

In the longitudinal driving simulation, the vehicle was driven at a fixed speed of 70 km/h, and the longitudinal driving conditions were separated into two: a flat (0%) and an inclined (30%) road driving. First, the road conditions of the vehicle driving longitudinally were set up at fixed intervals to check the power distribution system's control performance. To simulate the vehicle driving on a longitudinal incline, the experiments were performed at full throttle (100%) on a dry road with a 30% incline, which was the ground's maximum incline.

3.2.2. The Longitudinal Driving Simulation and HILS Experiment Results

Figure 7 illustrates the control output results of the power distribution system controller when the drive motor was operated at 20 and 100 rpm in flat (0%) road conditions. The control output maintained values between 40:60 and 60:40, which correspond to the front/rear power distribution ratios obtained by previous simulations. However, there was a time delay of approximately 0.02 s as the torque value output by the experiment equipment's torque sensor was inputted into the PC via the DAQ, and it was confirmed that oscillation occurred in the CarSim controller's output. Nevertheless, the error rate was less than 3%, and it is not expected to have a significant effect on control.

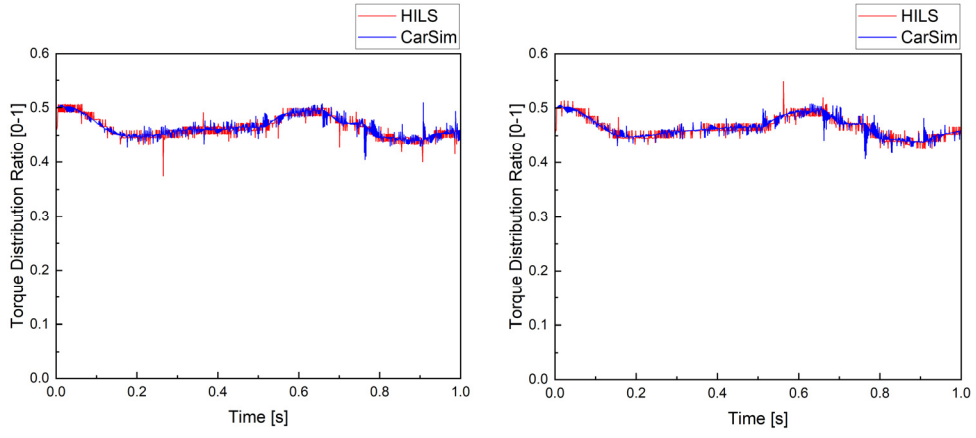

Figure 7. Power distribution ratio: (**a**) 20 rpm. (**b**) 100 rpm.

Figure 8 shows the front/rear driveshaft torque results according to the power distribution ratio based on the front/rear driveshaft torque values outputted by the CarSim vehicle when the output of the controller was inputted as the vehicle's rear-wheel driveshaft torque ratio. Owing to the characteristics of the program, the interval at 0–0.1 s was deemed to be an unstable interval. Therefore, the stabilized region from 0.2 to 1.0 s was analyzed. During the interval from 0.3–0.5 s, which indicates the moment when the frictional coefficient changed from $Mu = 0.5$ to $Mu = 0.2$, the front wheel experienced a relative loss of friction force, and the rear-wheel driveshaft torque increased by 11.06 Nm at 20 rpm and 6.34 Nm at 100 rpm to transmit additional power to the rear wheels. Moreover, when considering the front/rear driveshaft torque during the interval from 0.5–0.7 s, which corresponds to the moment when the friction coefficient changed from $Mu = 0.2$ to $Mu = 0.9$, there were torque differences of 43.22 Nm and 45.51 Nm, respectively. Even when the road's state varied rapidly, there was no significant impact on the power transmission.

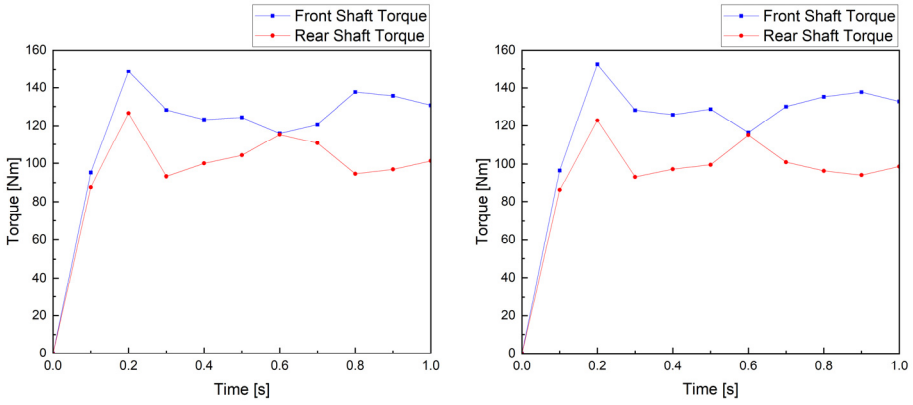

Figure 8. Front/rear driveshaft torque: (**a**) 20 rpm. (**b**) 100 rpm.

Figure 9 presents a graph that shows the longitudinal slip ratio of the wheels, and it confirms that the longitudinal slip ratio of the wheel's changed according to the rapid changes in the road friction coefficient. During the interval from 0.3–0.5 s, which corresponds to the instance when the friction coefficient changed from $Mu = 0.5$ to $Mu = 0.2$, the changes in the slip ratio at both 20 rpm and 100 rpm were not large. However, during the interval from 0.5–0.7 s, which corresponds to the instance when the friction coefficient changed from $Mu = 0.2$ to $Mu = 0.9$, there were momentary increases of 0.014907 and 0.014631, which are factors of 1.4 and 1.44, respectively, and they were found in the rear right wheel (RR). In addition, owing to the time delay, the rear right wheel's (RL) slip ratio output had a time delay of 0.1 s, and it was found that a slip ratio difference between the front wheel and the rear wheel occurred in the moments when the road friction coefficient changed.

Figure 10 illustrates the control output results of the power distribution system controller when the drive motor was operated at 20 rpm and 100 rpm on an inclined road (30%). Since the vehicle drove on a road with a fixed gradient of 30%, the CarSim controller's output was fixed at 0.6 after 0.175 s and 0.172 s, respectively. Furthermore, when the CarSim controller output was 0.5 or greater, the MR fluid multi-plate clutch changed to friction mode to transmit the required torque. Accordingly, it was determined that the sub-controller controlling the MR multi-plate clutch performed smoothly.

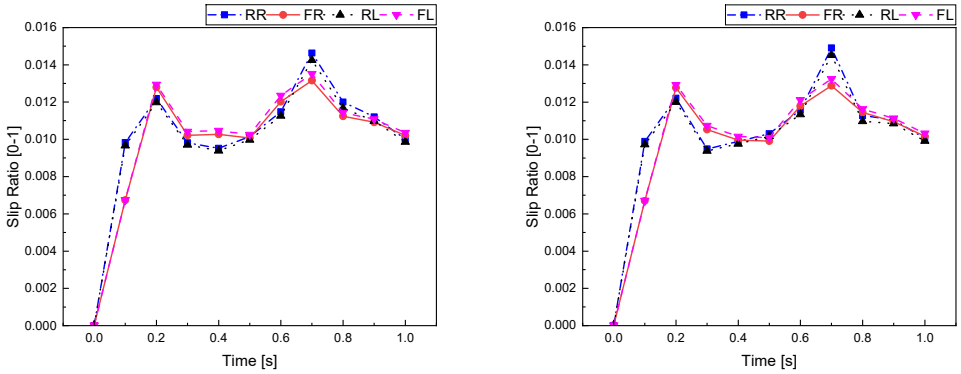

Figure 9. The wheel's longitudinal slip ratio: (**a**) 20 rpm. (**b**) 100 rpm.

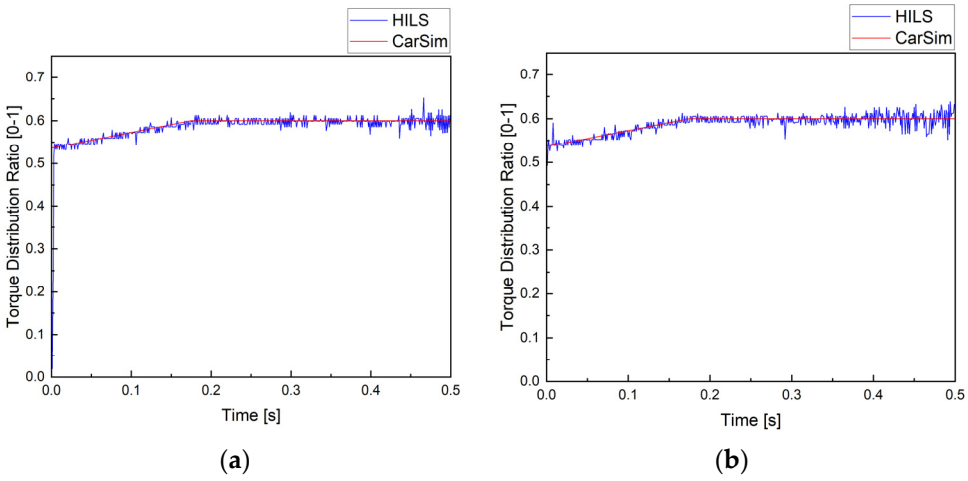

Figure 10. Power distribution ratio: (**a**) 20 rpm. (**b**) 100 rpm.

3.2.3. Lateral Driving Simulation Conditions

In the lateral driving simulation, the vehicle drove at a fixed speed of 70 km/h, and a DLC (double-lane change) was performed. The total length of the road was 60 m, and the frictional coefficient of the road was set at $Mu = 0.9$. Moreover, the initial power distribution ratio was set at 90:10 to clearly show the changes in lateral angular velocity.

3.2.4. The Lateral Driving Simulation and HILS Experiment Results

Figure 11 shows the control output results of the power distribution system controller during DLC driving when the power distribution ratio instantaneously changed from 90:10 to 70:30 while the RPM of the drive motor was 20 and 100 rpm. Accordingly, the CarSim controller outputted a relatively fixed value without any significant variations, and the results for the drive conditions of 20 and 100 rpm both exhibited similar trends with an error of ± 0.01, thus confirming proper adherence to the power distribution ratio.

Figure 12 illustrates the lateral acceleration and yaw rate of the vehicle during DLC driving. When the vehicle made a left turn, the lateral acceleration and yaw rate increased rapidly, and the lateral acceleration was +0.38 g′ and the yaw rate was +10.07 deg/s. When the vehicle made a right turn, there was a decreasing trend in which the lateral acceleration was -0.51 g′, and the yaw rate was -13.2 deg/s. Notably, identical results were also observed at 20 and 100 rpm, respectively.

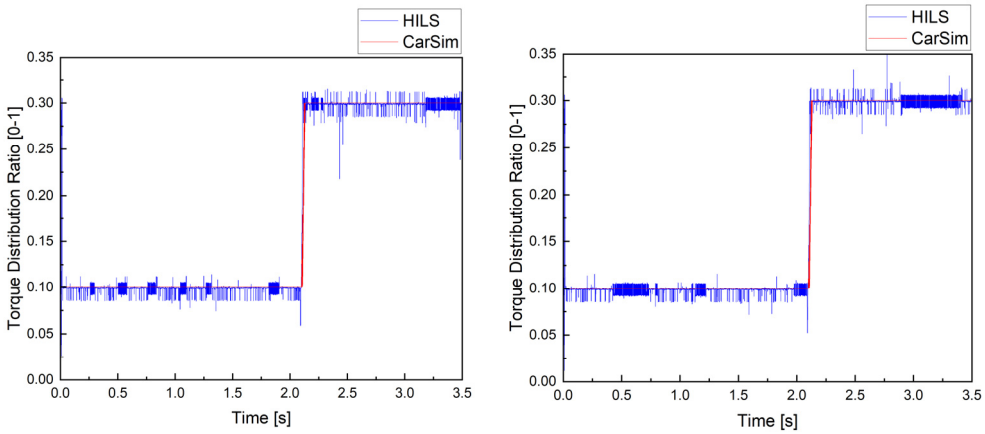

Figure 11. Power distribution ratio: (**a**) 20 rpm. (**b**) 100 rpm.

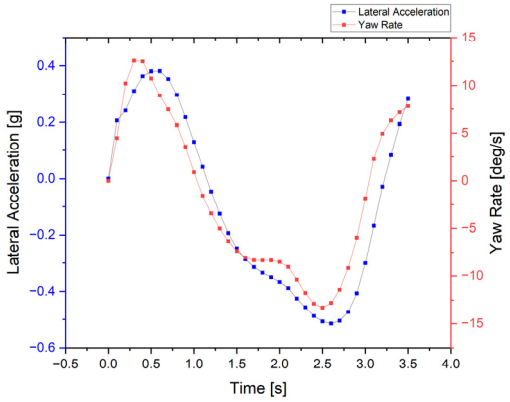

Figure 12. The vehicle lateral acceleration and yaw rate when DLC driving.

4. Conclusions

This study derived the torque modeling relationships for an MR fluid multi-plate clutch using MR fluid, and a HILS system was used to perform simulations and MR fluid multi-plate clutch link control.

The flow properties of the MR fluid were changed by applying a current and forming a magnetic field to control the ensuing torque transmission ratio. Consequently, a maximum transmission torque of 16.7 Nm was obtained in fluid mode, and the torque value increased in proportion to the current. Accordingly, it was determined that power transmission can be achieved by controlling the current.

A PID controller suitable for each driving condition was designed by receiving feedback regarding the dynamic changes in the vehicle in real time, and a HILS system was implemented via a co-simulation in CarSim and MATLAB/Simulink. As a result, a 0.02 s time delay occurred; however, the error rate was less than 3%. Therefore, it was deemed that smooth control is possible.

The front/rear driveshaft torque difference changed owing to the changes in the power distribution ratio according to the drive motor's rotation speed in the longitudinally flat (0%) road driving experiments. As such, the driveshaft rotation speed of the power distribution system affected the power distribution ratio by at least 2.29 Nm and a maximum of 4.72 Nm according to the road friction coefficient. However, it was determined that stable driving can be achieved because of the response to the power distribution ratio based on the fact that the change in the road friction coefficient was quick at less than 0.1 s.

In the lateral DLC driving experiments, the vehicle was unaffected by changes in the drive motor's RPM or the changes in the front/rear power distribution ratio when the

lateral acceleration and lateral angular velocity changed rapidly, and it was determined that smooth control is possible at a maximum lateral acceleration of 0.51 g and a maximum yaw rate of 13.2 deg/s.

A communications delay of 0.02 s occurred between the DAQ and the PC, which are components of the HILS system. It was also determined that unstable elements can be removed to ensure stable control by designing a digital controller that considers this time delay when conducting experiments.

Author Contributions: Conceptualization, J.-H.J. and J.-Y.P.; methodology, Y.-C.K.; software, J.-H.J.; validation, J.-Y.P., J.-H.J. and Y.-C.K.; formal analysis, J.-Y.P.; investigation, J.-H.J.; resources, Y.-C.K.; data curation, J.-Y.P.; writing—original draft preparation, J.-Y.P.; writing—review and editing, J.-Y.P.; visualization, J.-H.J.; supervision, Y.-C.K.; project administration, Y.-C.K.; funding acquisition, Y.-C.K. All authors have read and agreed to the published version of the manuscript.

Funding: These results were supported by the "Regional Innovation Strategy (RIS)" through the National Research Foundation of Korea (NRF), which is funded by the Ministry of Education (MOE) (2021RIS-004).

Institutional Review Board Statement: Not applicable.

Informed Consent Statement: Not applicable.

Data Availability Statement: The original contributions presented in the study are included in the article, further inquiries can be directed to the corresponding author.

Conflicts of Interest: Author Jin-Young Park was employed by the company EPSTech Co., Ltd. The remaining authors declare that the research was conducted in the absence of any commercial or financial relationships that could be construed as a potential conflict of interest.

References

1. Yim, S. Comparison among Active Front, Front Independent, 4-Wheel and 4-Wheel Independent Steering Systems for Vehicle Stability Control. *Electronics* **2020**, *9*, 798. [CrossRef]
2. Jauch, F. *Model-Based Application of a Slip-Controlled Converter Lock-Up Clutch in Automatic Car Transmissions*; SAE Technical Paper; SAE: Warrendale, PA, USA, 1999.
3. Gao, B.; Lei, Y.; Ge, A.; Chen, H.; Sanada, K. Observer-based clutch disengagement control during gear shift process of automated manual transmission. *Veh. Syst. Dyn.* **2011**, *49*, 685–701. [CrossRef]
4. Kim, T.S.; Kim, N.D.; Jang, J.D.; Kim, H.S. Development of Torque Converter Lock-up and Performance Simulator for Automatic Transmission Vehicle. In *Spring and Fall Conference of the Korean Society of Automotive Engineers*; Korean Society of Automotive Engineers: Seoul, Republic of Korea, 2007; Volume 2, pp. 946–951.
5. Kim, J.-M. Clutch Control of the Automated Manual Transmission for Smooth Gearshifting. Master's Thesis, Hanyang University Graduate School, Seoul, Republic of Korea, 2008.
6. Cho, J.; Kim, W.; Kim, W.; Jang, S. Characteristic Dynamics Torque Vibration of Behavior in Wet Clutch Engagement for Dual Clutch Transmissions. *Trans. Korean Soc. Automot. Eng.* **2016**, *24*, 183–190. [CrossRef]
7. Kim, B.W. A Study on Shift Control Method for Optimization of Jerking and Time of Agricultural Tractor with Hydraulic Clutch. Master's Thesis, Department of Electric Engineering Graduate School, Ulsan University, Ulsan, Republic of Korea, 2019.
8. Park, W.S. A Study on Torque Biasing Device Control for Longitudinal and Lateral Dynamic Performance Improvement. Master's Thesis, Hanyang University Graduate School, Seoul, Republic of Korea, 2012.
9. Wang, S.; Chen, F.; Tian, Z.; Li, A.; Wu, X. Design, experiment, and performance analysis of magnetorheological clutch with uniform magnetic field distribution along the radial direction for tension control. *Rev. Sci. Instrum.* **2021**, *92*, 125006. [CrossRef] [PubMed]
10. Wu, J.; Deng, B.; Huang, Y.; Zhang, H.; Tang, S. A multi-pole magnetorheological clutch powered by permanent magnets and excitation coils. *J. Intell. Mater. Syst. Struct.* **2022**, *34*, 217–228. [CrossRef]
11. Galvagno, E.; Dimauro, L.; Mari, G.; Velardocchia, M.; Vella, A.D. *Dual Clutch Transmission Vibrations during Gear Shift: A Simulation-Based Approach for Clunking Noise Assessment*; No. 2019-01-1553; SAE Technical Paper; SAE: Warrendale, PA, USA, 2019.
12. Thakur, M.K.; Sarkar, C. Experimental and Numerical Study of Magnetorheological Clutch with Sealing at Larger Radius Disc. *Def. Sci. J.* **2020**, *70*, 575–582. [CrossRef]
13. Singh, A.; Thakur, M.K.; Sarkar, C. Design and development of a wedge shaped magnetorheological clutch. *Proc. Inst. Mech. Eng. Part L J. Mater. Des. Appl.* **2020**, *234*, 1252–1266. [CrossRef]
14. Christie, M.; Sun, S.; Quenzer-Hohmuth, J.; Deng, L.; Du, H.; Li, W. A magnetorheological fluid based planetary gear transmission for mechanical power-flow control. *Smart Mater. Struct.* **2021**, *30*, 045013. [CrossRef]

15. Cirimele, V.; Dimauro, L.; Repetto, M.; Bonisoli, E. Multi-objective optimisation of a magnetic gear for powertrain applications. *Int. J. Appl. Electromagn. Mech.* **2019**, *60*, S25–S34. [CrossRef]
16. Filippini, M.; Torchio, R.; Alotto, P.; Bonisoli, E.; Dimauro, L.; Repetto, M. A New Class of Devices: Magnetic Gear Differentials for Vehicle Drivetrains. *IEEE Trans. Transp. Electrif.* **2022**, *9*, 2382–2397. [CrossRef]
17. Quoc, N.V.; Tuan, L.D.; Hiep, L.D.; Quoc, H.N.; Choi, S.B. Material Characterization of MR Fluid on Performance of MRF Based Brake. *Front. Mater.* **2019**, *6*, 125. [CrossRef]
18. Nguyen, P.B.; Choi, S.B. Accurate torque control of a bi-directional magneto-rheological actuator considering hysteresis and friction effects. *Smart Mater. Struct.* **2013**, *22*, 055002. [CrossRef]
19. Park, J.-Y.; Kim, G.-W.; Oh, J.-S.; Kim, Y.-C. Hybrid multi-plate magnetorheological clutch featuring two operating modes: Fluid coupling and mechanical friction. *J. Intell. Mater. Syst. Struct.* **2021**, *32*, 1537–1549. [CrossRef]
20. Ham, H.; Lee, H. Control Strategy Development of 4WD Vehicles based on Heuristic Approach and Dynamic Characteristic. *Trans. Korean Soc. Automot. Eng.* **2013**, *21*, 209–217. [CrossRef]
21. Zhu, C. Dynamic performance of a disk-type magnetorheological fluid damper under AC excitation. *J. Intell. Mater. Syst. Struct.* **2005**, *16*, 449–461. [CrossRef]
22. Park, J.-Y.; Kim, Y.-C.; Oh, J.-S.; Jeon, J.-H.; Jeong, J.-H. Optimal Design of Multi-Plate Clutch Featuring MR Fluid. *J. Korea Acad. Ind. Coop. Soc.* **2020**, *21*, 77–83.
23. Chooi, W.W.; Oyadiji, S.O. Design, modelling and testing of magnetorheological (MR) dampers using analytical flow solutions. *Comput. Struct.* **2007**, *86*, 473–482. [CrossRef]
24. Zhu, X.; Jing, X.; Cheng, L. Magnetorheological fluid dampers: A review on structure design and analysis. *J. Intell. Mater. Syst. Struct.* **2012**, *23*, 839–873. [CrossRef]
25. Hao, H.; Lu, T.; Zhang, J.; Zhou, B. A new control strategy of the filling phase for wet dual clutch transmission. *Proc. Inst. Mech. Eng. Part C J. Mech. Eng. Sci.* **2015**, *230*, 2013–2027. [CrossRef]
26. Törőcsik, D. Some design issues of multi-plate magnetorheological clutches. *Hung. J. Ind. Chem.* **2011**, *39*, 41–44.
27. Iqbal, S.; Al-Bender, F.; Ompusunggu, A.P.; Pluymers, B.; Desmet, W. Modeling and analysis of wet friction clutch engagement dynamics. *Mech. Syst. Signal Process.* **2015**, *60–61*, 420–436. [CrossRef]
28. Yamakawa, J.; Watanabe, K. A method of optimal wheel torque determination for independent wheel drive vehicles. *J. Terramechanics* **2006**, *43*, 269–285. [CrossRef]
29. Osborn, R.P.; Shim, T. Independent control of all-wheel-drive torque distribution. *Veh. Syst. Dyn.* **2006**, *44*, 529–546. [CrossRef]
30. Kang, D.H.; Lee, J.H.; Kim, S.S. Effects of Driving Torque Distribution of 4WD Vehicle on Handling Performance. In Proceedings of the KSAE 2009 Annual Conference, Pyeongchang, Republic of Korea, 4–6 November 2009; pp. 1000–1007.